Hrd1-ERAD controls the hepatokine FGF21 production through CREBH polyubiquitination

Juncheng Wei [1], Lu Chen [2], Fei Li [1], Yanzhi Yuan [3], Yajun Wang [1], Wanjun Xia [4], Yuehui Zhang [3], Yuanming Xu [1], Zhao Yang [5], Beixue Gao [1], Chaozhi Jin [3], Johanna Melo-Cardenas [1], Richard M. Green [7], Hui Pan [2,8], Jian Wang [3,8], Fuchu He [3,8], Kezhong Zhang [5,8] and Deyu Fang [1,6,8]

Appendix Figures S1 - S10 and Legends:

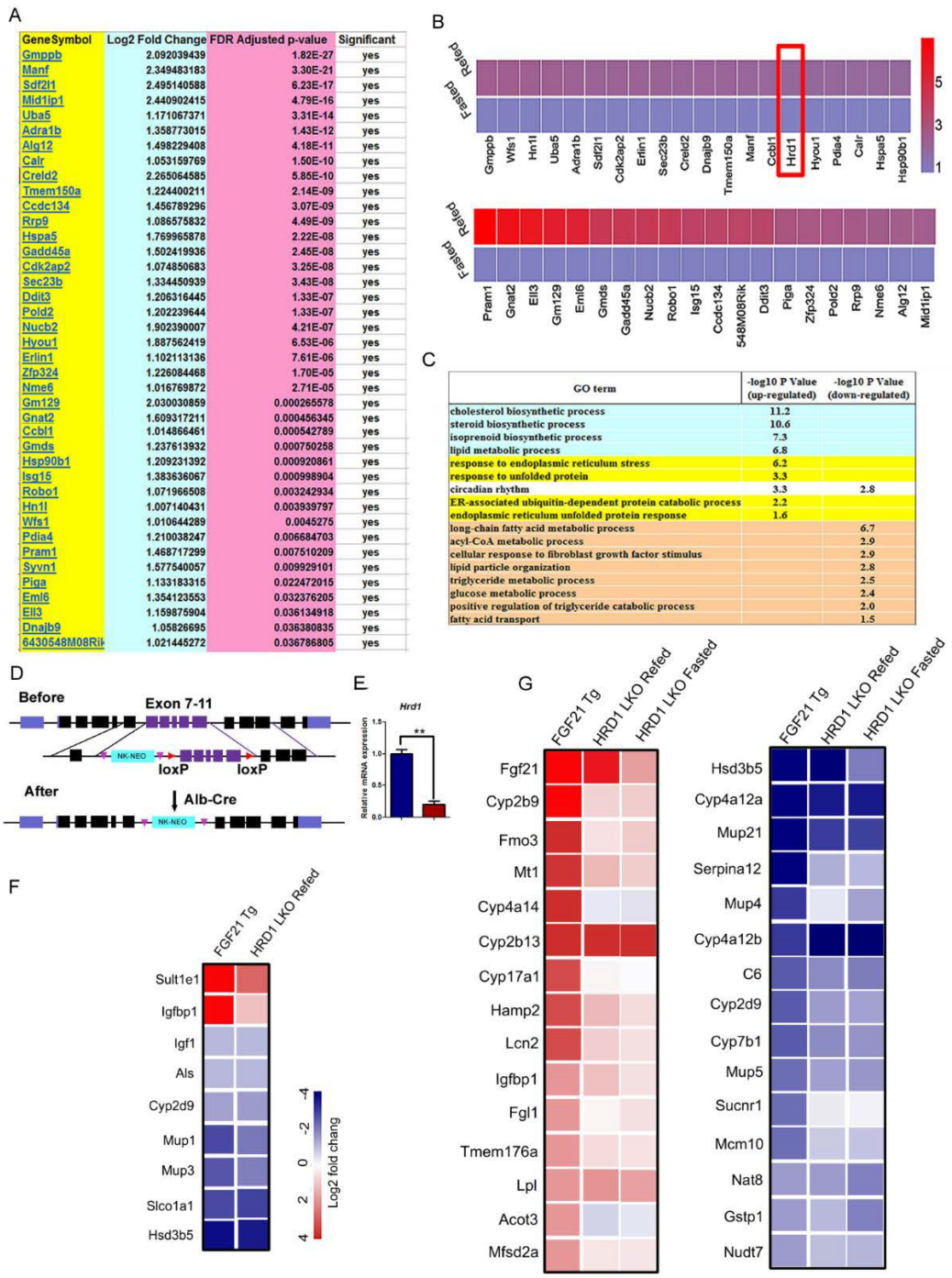

GeneSymbol	Log2 Fold Change	FDR Adjusted p-value	Significant
Gmppb	2.092039439	1.82E-27	yes
Manf	2.349483183	3.30E-21	yes
Sdf2l1	2.495140588	6.23E-17	yes
Mid1ip1	2.440902415	4.79E-16	yes
Uba5	1.171067371	3.31E-14	yes
Adra1b	1.358773015	1.43E-12	yes
Alg12	1.498229408	4.18E-11	yes
Calr	1.053159769	1.50E-10	yes
Creld2	2.265064585	5.85E-10	yes
Tmem150a	1.224400211	2.14E-09	yes
Ccdc134	1.456789296	3.07E-09	yes
Rrp9	1.086575832	4.49E-09	yes
Hspa5	1.769965878	2.22E-08	yes
Gadd45a	1.502419936	2.45E-08	yes
Cdk2ap2	1.074850683	3.25E-08	yes
Sec23b	1.334450939	3.43E-08	yes
Ddit3	1.206316445	1.33E-07	yes
Pold2	1.202239644	1.33E-07	yes
Nucb2	1.902390007	4.21E-07	yes
Hyou1	1.887562419	6.53E-06	yes
Erlin1	1.102113136	7.61E-06	yes
Zfp324	1.226084468	1.70E-05	yes
Nme6	1.016769872	2.71E-05	yes
Gm129	2.030030859	0.000265578	yes
Gnat2	1.609317211	0.000456345	yes
Ccbl1	1.014866461	0.000542789	yes
Gmds	1.237613932	0.000750258	yes
Hsp90b1	1.209231392	0.000920861	yes
Isg15	1.383636067	0.000998904	yes
Robo1	1.071966508	0.003242934	yes
Hn1l	1.007140431	0.003939797	yes
Wfs1	1.010644289	0.0045275	yes
Pdia4	1.210038247	0.006684703	yes
Pram1	1.468717299	0.007510209	yes
Syvn1	1.577540057	0.009929101	yes
Piga	1.133183315	0.022472015	yes
Eml6	1.354123553	0.032376205	yes
Ell3	1.159875904	0.036134918	yes
Dnajb9	1.05826695	0.036380835	yes
6430548M08Rik	1.021445272	0.036786805	yes

GO term	-log10 P Value (up-regulated)	-log10 P Value (down-regulated)
cholesterol biosynthetic process	11.2	
steroid biosynthetic process	10.6	
isoprenoid biosynthetic process	7.3	
lipid metabolic process	6.8	
response to endoplasmic reticulum stress	6.2	
response to unfolded protein	3.3	
circadian rhythm	3.3	2.8
ER-associated ubiquitin-dependent protein catabolic process	2.2	
endoplasmic reticulum unfolded protein response	1.6	
long-chain fatty acid metabolic process		6.7
acyl-CoA metabolic process		2.9
cellular response to fibroblast growth factor stimulus		2.9
lipid particle organization		2.8
triglyceride metabolic process		2.5
glucose metabolic process		2.4
positive regulation of triglyceride catabolic process		2.0
fatty acid transport		1.5

Appendix Fig S1. Generation of liver specific HRD1 knock-out mice. (A) ER stress target genes that are increased upon refeeding. (**B**) Hepatic mRNA profile in the fasting and refeeding condition. **(C)** Gene ontology analyzes the function of the up-regulated and down-regulated genes upon fasting and refeeding **(D)** Structure of the HRD1 WT and targeted alleles. **(E)** Hepatic mRNA level of the HRD1 LKO and WT mice. **(F)** Heatmaps of top 15 increased and decreased genes in FGF21 transgenic overexpression mice compared with HRD1 LKO mice in fasting and refeeding condition. (**G**) Growth hormone- STAT5 target genes in FGF21 transgenic overexpression mice and HRD1 LKO mice. *: $P<0.05$. **: $P<0.01$ by unpaired student's t test.

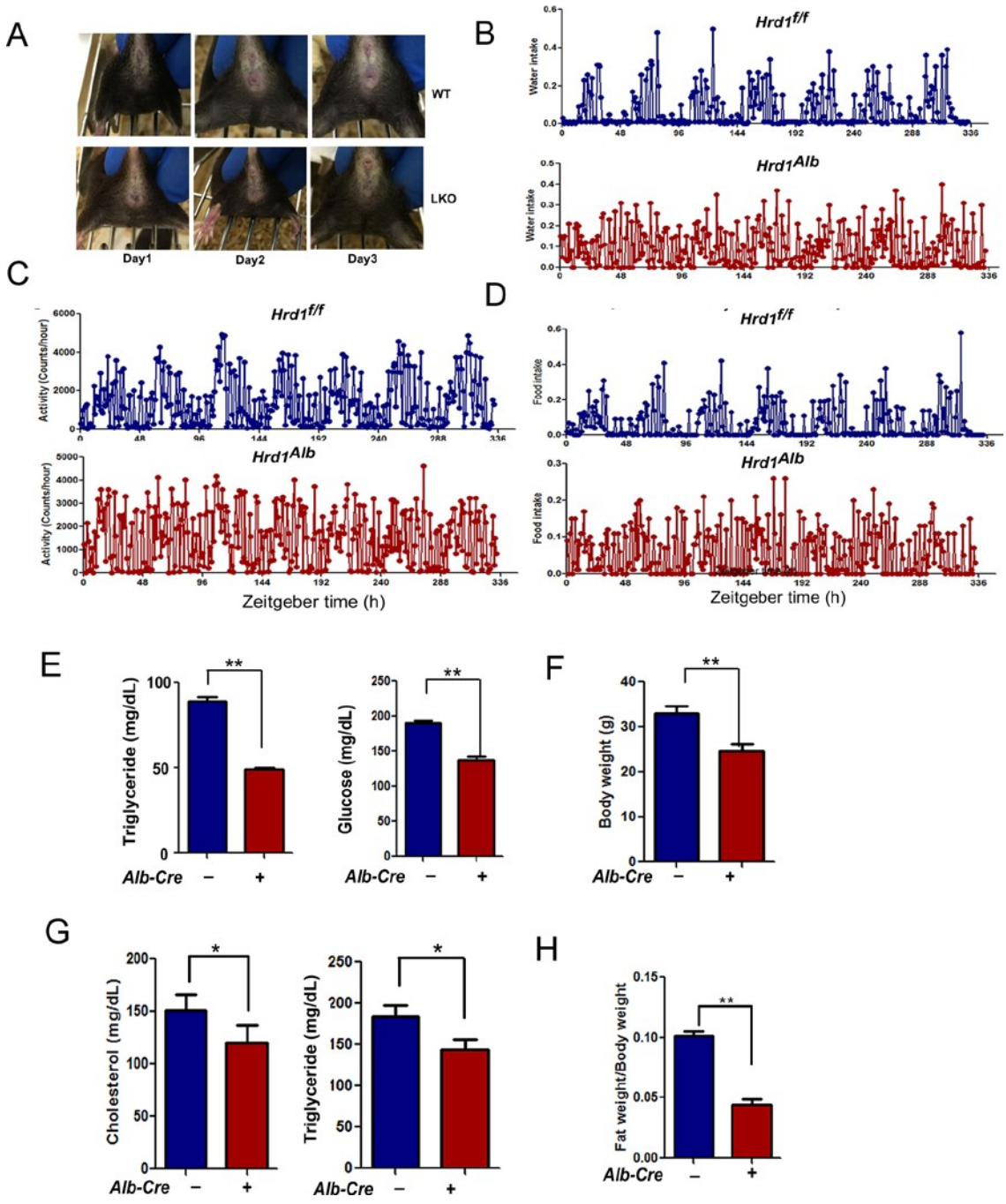

Appendix Fig S2. Hepatic HRD1 ablation mice phenocopy Fgf21 gain of function mice. (A) Evaluation the estrus cycle by the vaginal visual method. (**B-D**) Water intake, activity and feeding behaviors in the WT and L-HRD1 mice. (n=5 for each group). (**E**) Serum TG and blood glucose of WT and HRD1 LKO mice under refed conditions. (n=5 for each group). (**F-H**) Body weights (**F**), Cholesterol and TG (**G**), Fat weight and body weight ratio (n=5 for each group). (**H**) of WT and HRD1 LKO mice 16 weeks after HFD feeding (n=6 for each group). The data are representative of three independent experiments (mean ± s.d.). *: $P<0.05$. **: $P<0.01$ by unpaired student's t test.

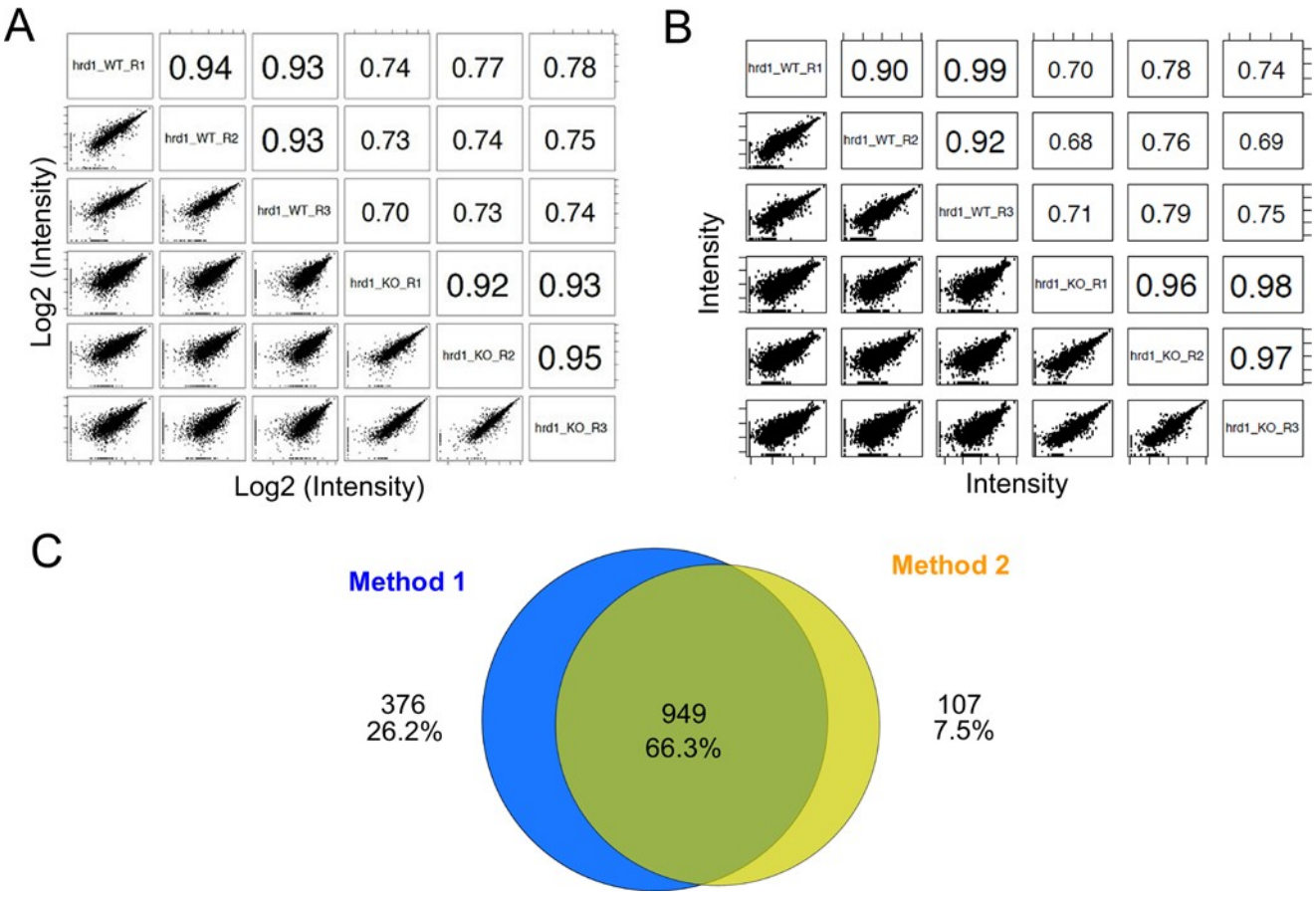

Appendix Fig S3. Data analysis of the proteomic differential proteins between WT and HRD1 LKO mice. (**A**) Correlation analysis of proteomic data from WT and HRD1 LKO livers with logarithmic-transformed intensity of proteins. (**B**) Correlation analysis of proteomic data from WT and HRD1 LKO livers with original intensity of proteins. (**C**) Overlaps of the differentially expressed proteins between the missing values replaced with 1 (method 1) and replaced with minimum value of each replicate (method 2).

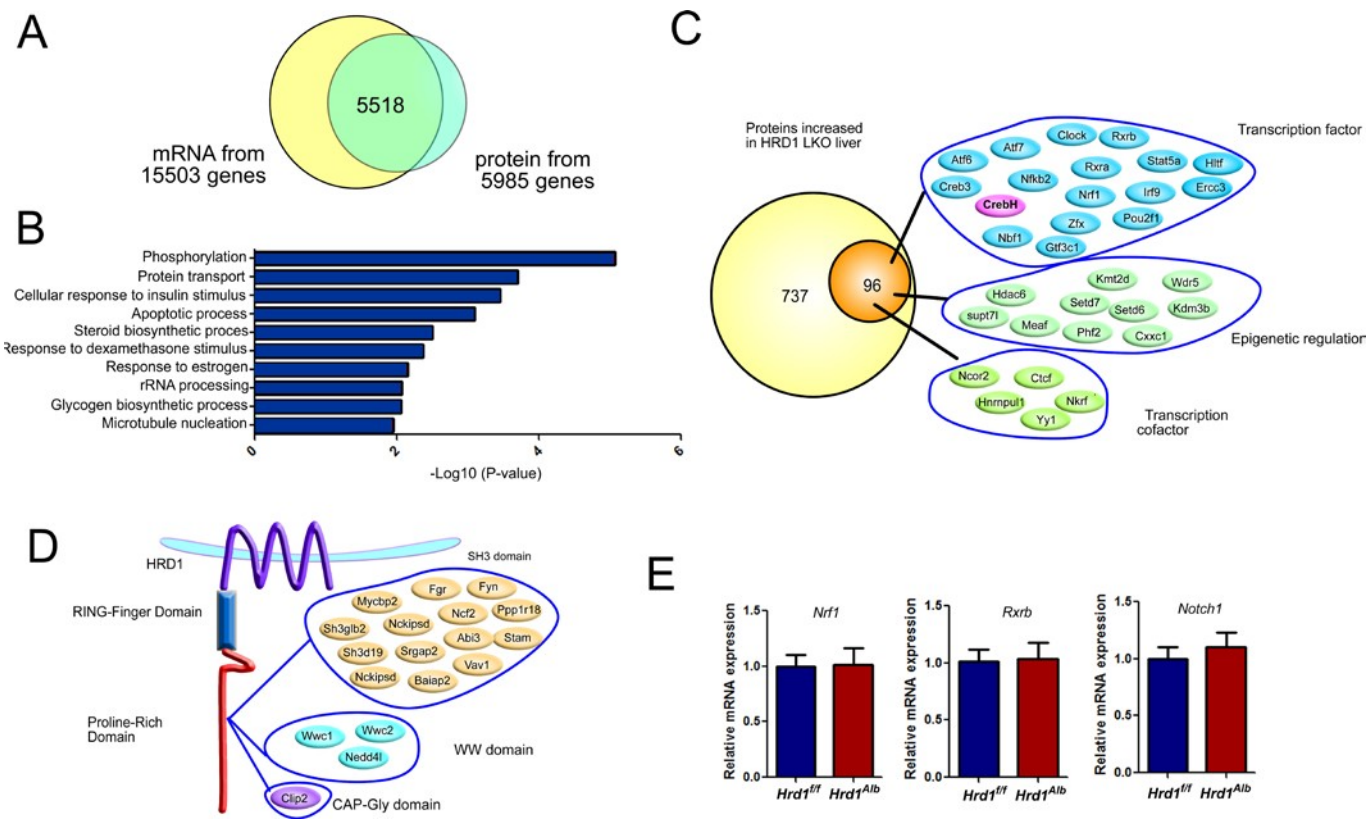

Appendix Fig S4. Candidate HRD1 substrates are identified by protein level enrichment (**A**) Correlation analysis of proteomic data from WT and HRD1 LKO livers. (**B**) Overlap of the genes identified between RNA-Seq and proteomics. (**C**) GO functional analysis of the differential proteins from proteomic screening. (**D**) 96 of the increased proteins directly regulate transcription. (**E**) Up-regulated proteins which contain the proline-line rich binding domain. (**F**) mRNA levels of IRE1α, NRF1, RXRβ, NOTCH1, SIRT3 and GAPDH in the liver of WT and HRD1 LKO mice under the refed condition. (n=6 for each group). The data are representative of three independent experiments (mean ± s.d.). *: P<0.05. **: P<0.01 by unpaired student's t test.

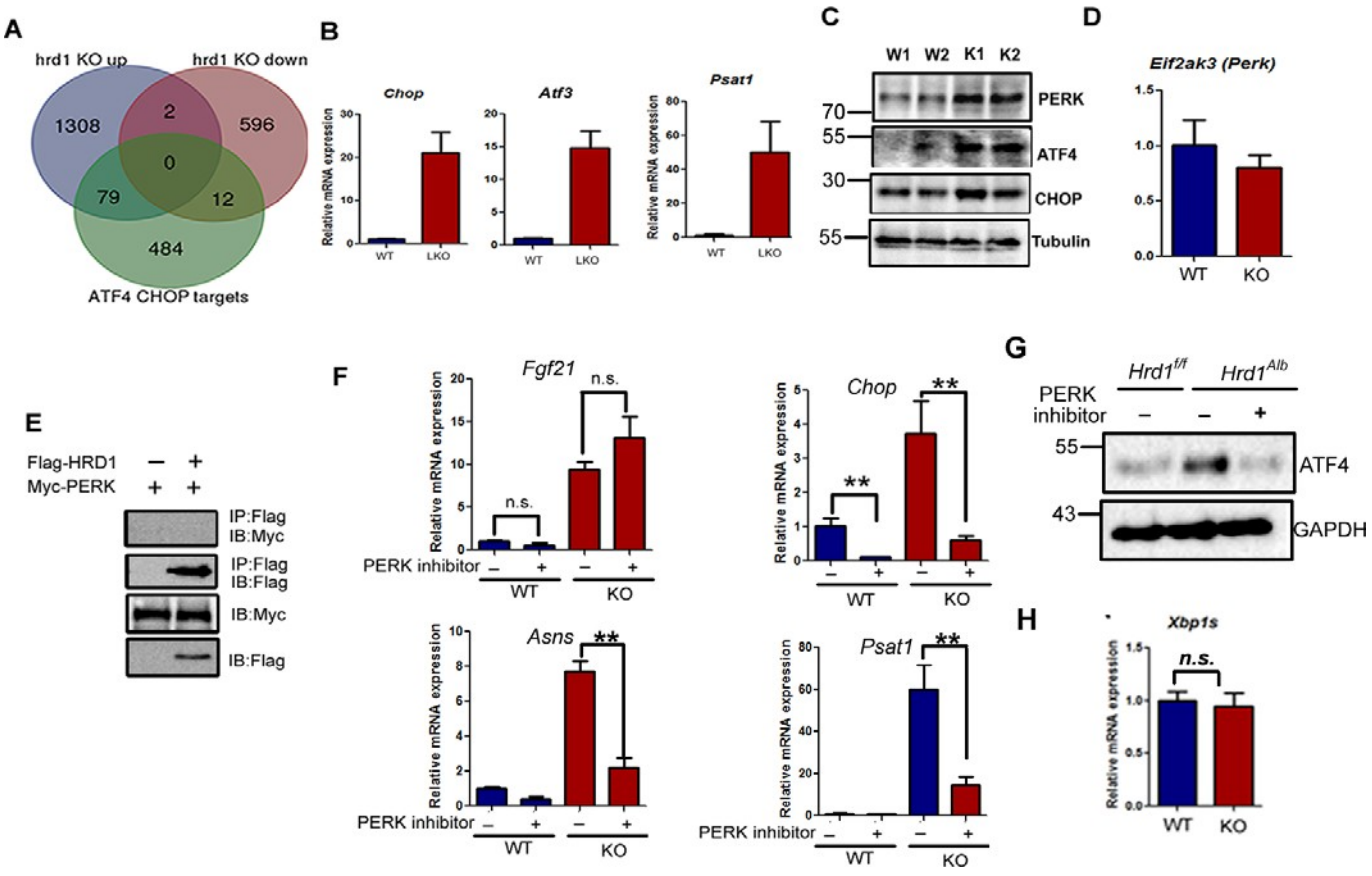

Appendix Fig S 5. (A) Overlap between HRD1 regulating genes and CHOP-ATF4 target genes. **(B)** Hepatic *Chop, Atf3* and *Psat1* mRNA levels in the WT and HRD1 LKO mice. (n=5 for each group). **(C)** Hepatic PERK, ATF4 and CHOP protein levels in the WT and HRD1 LKO mice. **(D)** Hepatic mRNA level of *Eif2ak3* (PERK). (n=5 for each group). **(E)** Western Blot analysis interaction of PERK and HRD1 after immunoprecipitates of Flag-agarose in transfected HEK293T. **(F)** *Fgf21* and *Chop*, *Asns* and *Psat1* mRNA expression after PERK inhibitor injection. (n=5 for each group). (**G**) ATF4 protein levels after PERK inhibitor injection. (n=5 for each group). (**H**) Xbp1s mRNA levels in WT and HRD1 KO mice. (n=5 for each group). The data are representative of three independent experiments (mean ± s.d.). *: $P<0.05$. **: $P<0.01$ by unpaired student's t test.

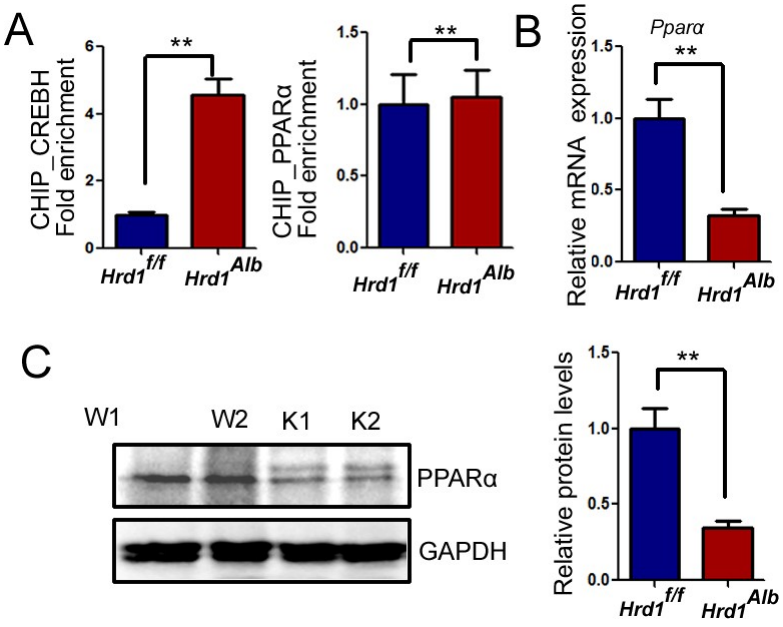

Appendix Fig S6. (A) Chromatin immunoprecipitation analysis of Crebh and PPARα binding onto the Fgf21 promoter in the livers of 12-weeksold mice, normalized first to 5% input group. (n=5 for each group). **(B)** Hepatic *Chop, Atf3* and *Psat1* mRNA levels in the WT and HRD1 LKO mice. (n=5 for each group). **(C)** Hepatic mRNA level of *Ppara*. (n=5 for each group). **(C)** Hepatic PPARα protein levels in the WT and HRD1 LKO mice. The data are representative of three independent experiments (mean ± s.d.). *: $P<0.05$. **: $P<0.01$ by unpaired student's t test.

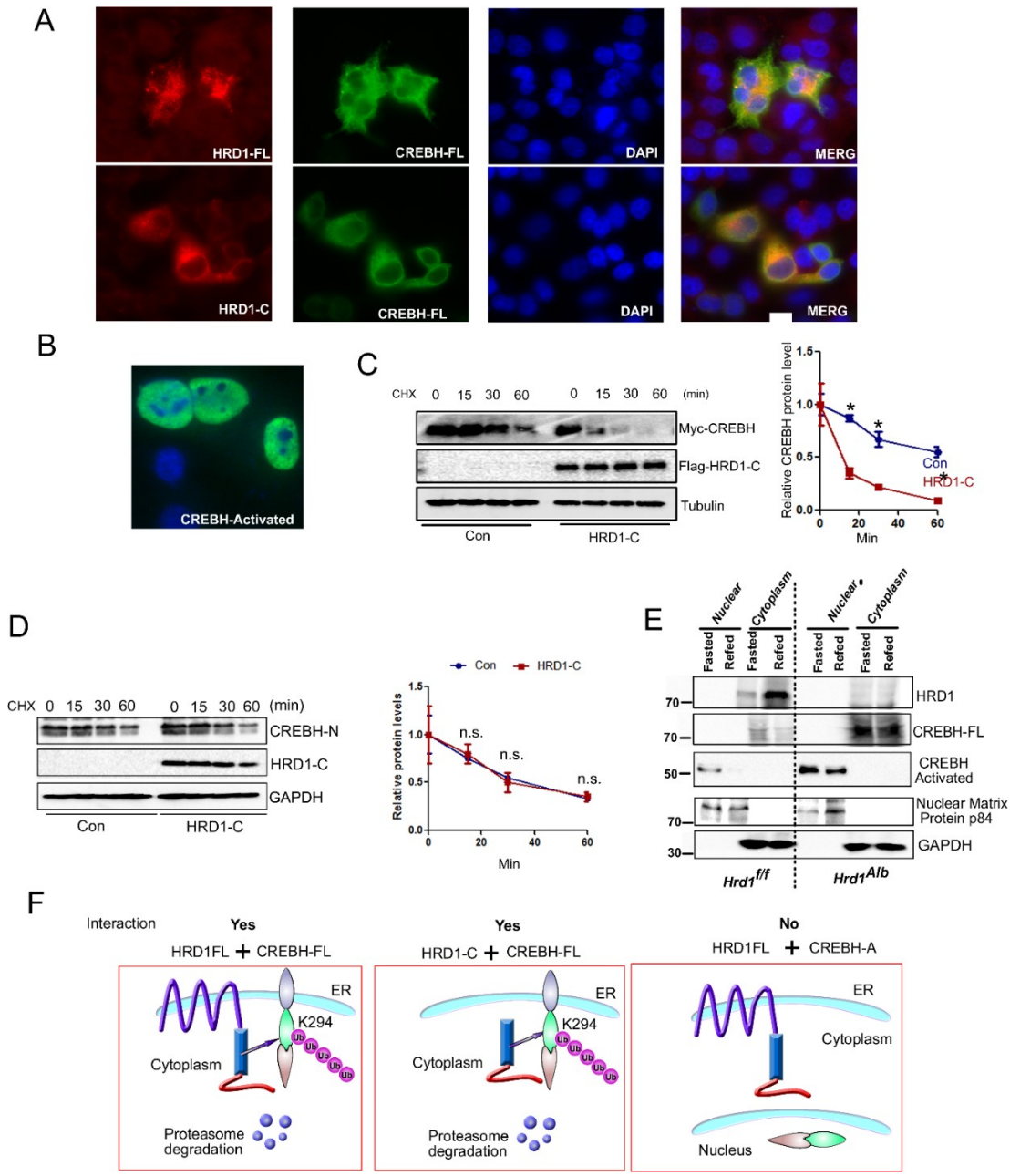

Appendix Fig S7. (A) Immunostaining of Flag-HRD1-C, Flag-HRD1 full-length and Myc-CREBH full-length 48 hours after transfection. **(B)** Immunostaining of Flag-CREBH-activated 48 hours after transfection. **(C-D)** Western Blot analysis cleaved form CREBH protein stability after HRD1-C terminal protein over-expression with CREBH full-length (**C**) CREBH-cleaved form (**D**). **(E)** Western blot analysis of hepatic HRD1 and CREBH of 16-weeks-old mice under overnight fasted or overnight fasted-refed 4 hours states; tissues were fractionated into nuclear and cytoplasm fractions. **(F)** A model of interaction between HRD1 and CREBH.

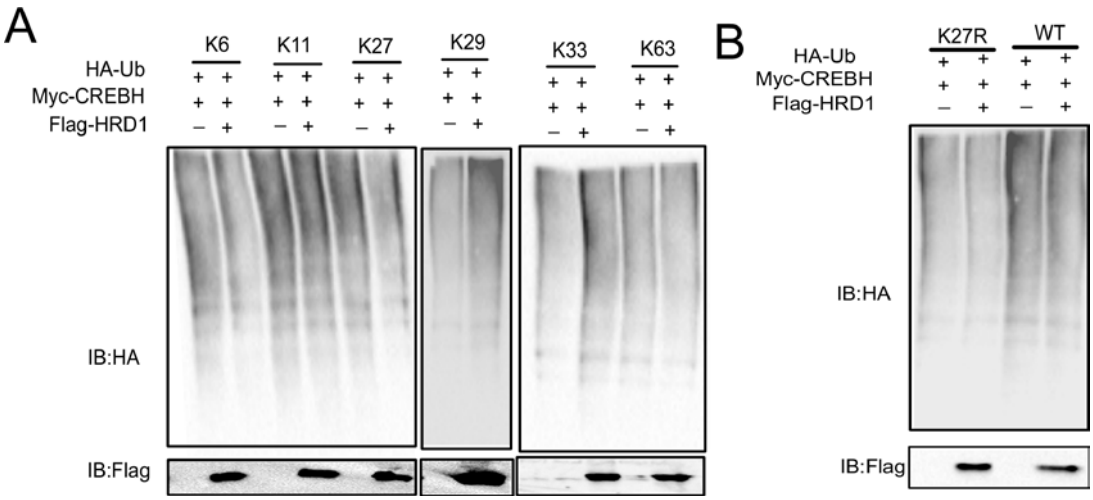

Appendix Fig S8. (**A**) Western Blot analysis of the CREBH K6, K11, K27, K29 and K33 only ubiquitination level after HRD1 co-expression. (**B**) Western Blot analysis of the CREBH WT, K27R ubiquitination level after HRD1 full-length co-expression.

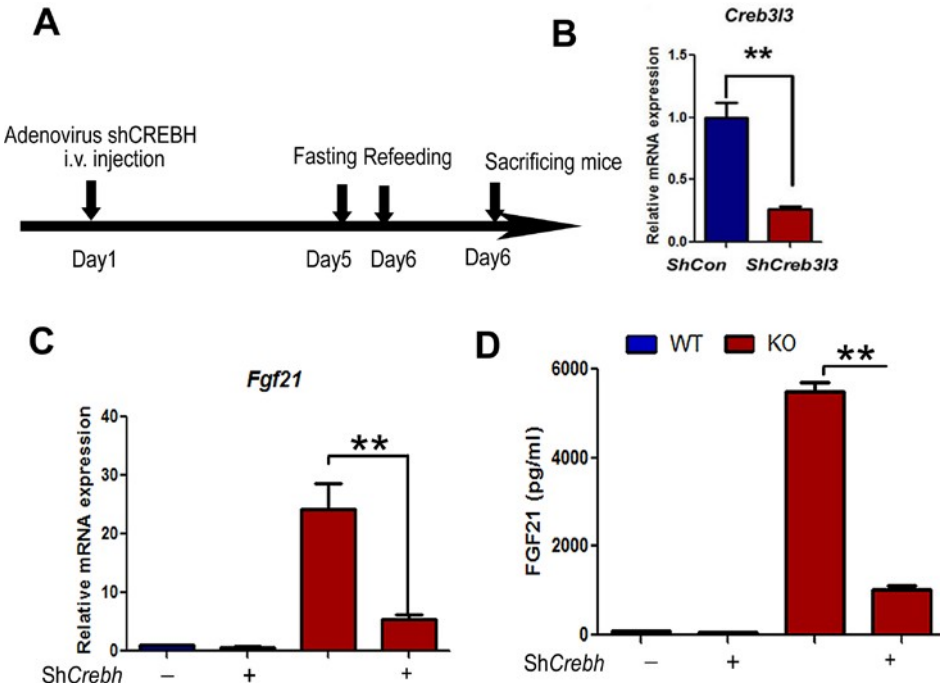

Appendix Fig S9. (**A**) Flowchart of the study design for the knockdown CREBH in vivo. (**B-C**) Hepatic Crebh and Fgf21 mRNA in the WT and L-HRD1 KO mice 5 days after *Crebh* shRNA adenovirus injection. (**C**) Serum FGF21 protein levels in the WT and L-HRD1 KO mice 5 days after *Crebh* shRNA adenovirus injection. *: $P<0.05$. **: $P<0.01$ by unpaired student's t test.

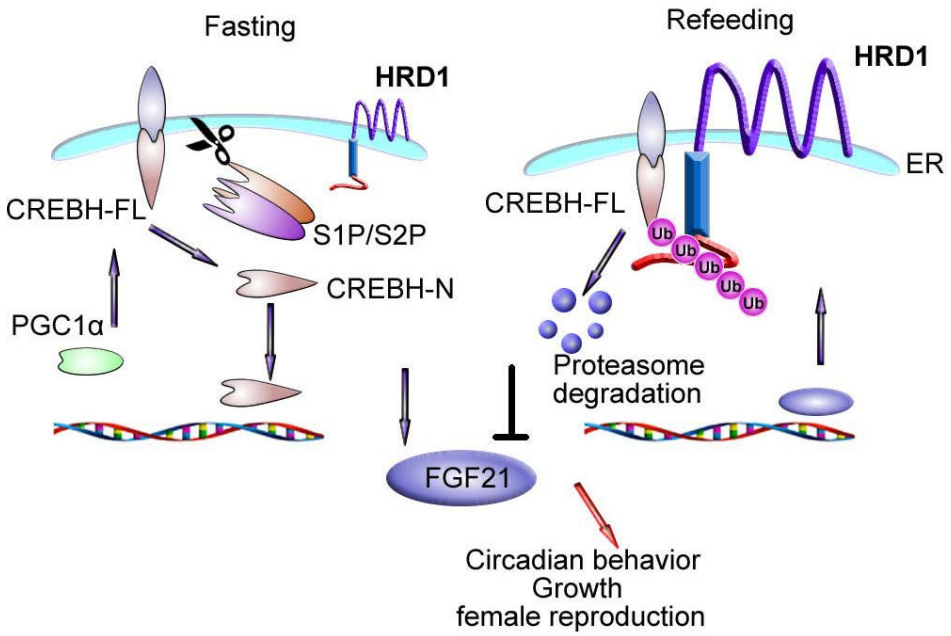

Appendix Fig S10. A working model how HRD1 control FGF21 expression in the fasting-refeeding condition